J Mol Model (2012) 18:103–114
DOI 10.1007/s00894-011-1040-5

ORIGINAL PAPER

# Computer-assisted design for paracetamol masking bitter taste prodrugs

**Hatem Hejaz · Rafik Karaman · Mustafa Khamis**

Received: 30 January 2011 / Accepted: 14 March 2011 / Published online: 15 April 2011


**Abstract** It is believed that the bitter taste of paracetamol, a pain killer drug, is due to its hydroxyl group. Hence, it is expected that blocking the hydroxy group with a suitable linker could inhibit the interaction of paracetamol with its bitter taste receptor/s and hence masking its bitterness. Using DFT theoretical calculations we calculated proton transfers in ten different Kirby's enzyme models, 1–10. The calculation results revealed that the reaction rate is linearly correlated with the distance between the two reactive centers ($r_{GM}$) and the angle of the hydrogen bonding ($\alpha$) formed along the reaction pathway. Based on these results three novel tasteless paracetamol prodrugs were designed and the thermodynamic and kinetic parameters for their proton transfers were calculated. Based on the experimental $t_{1/2}$ (the time needed for the conversion of 50% of the reactants to products) and EM (effective molarity) values for processes 1–10 we have calculated the $t_{1/2}$ values for the conversion of the three prodrugs to the parental drug, paracetamol. The calculated $t_{1/2}$ values for ProD 1–3 were found to be 21.3 hours, 4.7 hours and 8 minutes, respectively. Thus, the rate by which the paracetamol prodrug undergoes cleavage to release paracetamol can be determined according to the nature of the linker of the prodrug (Kirby's enzyme model 1–10). Further, blocking the phenolic hydroxyl group by a linker moiety is believed to hinder the paracetamol bitterness.

**Keywords** DFT calculations · Kirby's enzyme models · Masking bitter taste · Paracetamol prodrugs · Proton transfer reaction

**Electronic supplementary material** The online version of this article (doi:10.1007/s00894-011-1040-5) contains supplementary material, which is available to authorized users.

H. Hejaz · R. Karaman (✉)
Faculty of Pharmacy, Al-Quds University,
P. O. Box 20002, Jerusalem, Palestine
e-mail: dr_karaman@yahoo.com

M. Khamis
Department of Chemistry and Chemical Technology,
Al-Quds University,
P. O. Box 20002, Jerusalem, Palestine

## Introduction

Bitter or unpleasant taste is a major problem in the food and medicine industries. As several oral pharmaceuticals and bulking agents have unpleasant, bitter-tasting components, Pediatric patients resists taking medicine due to their bitterness or unpleasant taste. The bitterness of these preparations leads to lack of patient compliance. The problem of bitterness of drugs in pediatric and geriatric formulations is creating a serious challenge to pharmacists [1].

The desire of improved palatability in bitter taste products has prompted the development of numerous formulations with improved performance and acceptability [2]. In order to satisfy the patient compliance for taking medicines bitterness masking becomes essential. Different approaches are commonly utilized to overcome bitter and unpleasant taste of drugs. This includes reduction of drug solubility in saliva, where a balance between reduced solubility and bioavailability must be achieved, but these approaches were found to be limited and could not overcome the problem of bitterness [3]. Thus, different strategies should be developed in order to overcome this serious problem.

Drugs or molecules interact with taste receptors on the tongue to give bitter, sweet or other taste sensations. Altering the ability of the drug to interact with taste

receptors could reduce or eliminate their bitterness. This could be achieved by an appropriate modification of the structure and the size of a bitter compound.

During the last ten years, tremendous progress in the elucidation of bitter taste reception and transduction on the cellular level was made and many new molecules and compounds to reduce off-taste were reported, but none of those were found to eliminate the bitterness fully [4].

Since the discovery and identification of the receptor proteins responsible for bitter taste reception, the mechanism of bitter reception by taste receptor cells seems to be generally known nowadays. Bitter molecules bind to G-protein coupled receptor-type T2R on the apical membrane of the taste receptor cells located in the taste buds. In humans, about 25 different T2R are described. Additionally, several alleles are known and about 1000 different bitter phenotypes exist in human beings [4, 5].

Due to the wide variation of the structure basis of bitter tasting molecules, it is difficult to generalize the molecular requirements for bitterness. Nevertheless, it was noted that a bitter molecule needs a polar group and a hydrophobic moiety (mono polar-hydrophobic concept). A quantitative structure activity relationship (QSAR) model was developed and could be established for the prediction of bitterness of several analogues. For example, it was reported that an addition of pyridinium moiety to an amino acid chain of a variety of bitter amino acids compounds decreases the bitterness such as in the case of glycine (e.g., pyridinium glycinyl betain). Other structural modifications such as an increase in the number of amino groups/residues to more than three and a reduction in the poly-hydroxyl group/ COOH has been proven to decrease the bitterness in a significant manner. Furthermore, changing the configuration of bitter compounds by preparing isomer analogues was found to be important for binding affinity to enhance bitterness agonist activity (e.g., L-tryptophan is bitter while D-tryptophan is sweet, and there are many other examples) [4, 6].

Paracetamol is an odorless crystalline compound with a bitter taste widely used as pain killer and to reduce the temperature of patients with fever. These actions are known respectively as analgesic and antipyretic. Initially, paracetamol was found in the urine of patients who had taken phenacetin and later on it was demonstrated that paracetamol was a urinary metabolite of acetanilide [7].

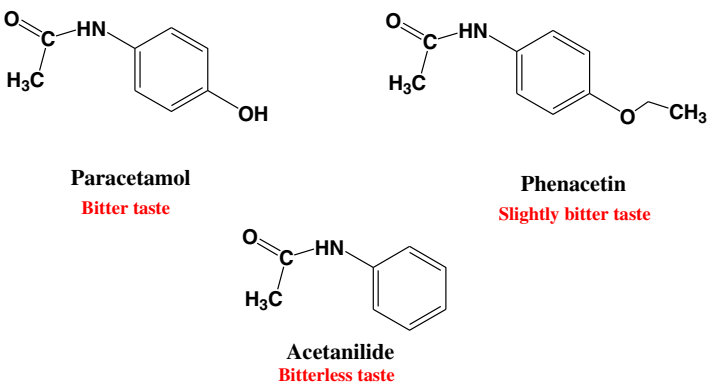


Phenacetin, on the other hand, lacks or has a very slight bitter taste [8]. Examination of the structures of paracetamol and phenacetin reveals that the only difference in the structural features in both is the nature of the group on the *para* position of the benzene ring. While in the case of paracetamol the group is hydroxy, in phenacetin it is ethoxy. Another related example is acetanilide that has a chemical structure similar to that of paracetamol and phenacetin but it lacks the group in the *para* position of the benzene ring. Acetanilide has a burning taste and lacks the bitter taste characteristic for paracetamol [9]. The combined facts described above suggest that the presence of hydroxy group on the *para* position is the major contributor for the bitter taste of paracetamol. Hence, it is expected that blocking the hydroxy group in paracetamol with a suitable linker could inhibit the interaction of paracetamol with its bitter taste receptor/s and hence masking its bitterness.

It seems reasonable to assume that the phenolic hydroxyl group in paracetamol is crucial for obtaining the bitter taste characteristic for paracetamol. This might be due to the ability of paracetamol to be engaged in a hydrogen bonding net with the active site of its bitter taste receptor *via* its phenolic hydroxyl group.

Recently we have been researching the mechanistic pathways of some intramolecular processes that have been used as enzyme models and prodrug linkers [10–27]. Utilizing DFT and *ab initio* molecular orbital calculation

methods, we have studied: 1) (a) acid-catalyzed lactonization of hydroxy-acids as investigated by Cohen [28–30] and Menger [31–38], (b) $S_N2$-based-cyclization reactions of dicarboxylic semi-esters to yield anhydrides as studied by Bruice [39, 40], (c) intramolecular $S_N2$-based ring-closing reactions as researched by Brown's group [41] and Mandolini's group [42], (d) proton transfer between two oxygens in Kirby's acetals [43–52], and proton transfer between nitrogen and oxygen in Kirby's enzyme models [43–52], (e) proton transfer between two oxygens in rigid systems as investigated by Menger [31–38], and (f) proton transfer from oxygen to carbon in some of Kirby's enol ethers [43–52] arriving at the following conclusions. (1) The driving force for enhancements in rate for intramolecular processes are both entropy and enthalpy effects. In the cases by which enthalpic effects were predominant such as ring-cyclization and proton transfer reactions proximity or/and steric effects were the driving force for rate accelerations. (2) The nature of the reaction being intermolecular or intramolecular is determined on the distance between the two reactive centers. (3) In $S_N2$-based ring-closing reactions leading to three-, four- and five-membered rings the *gem*-dialkyl effect is more dominant in processes involving the formation of an unstrained five-membered ring, and the need for directional flexibility decreases as the size of the ring being formed increases. (4) Accelerations in the rate for intramolecular reactions are a result of both entropy and enthalpy effects. (5) An efficient proton transfer between two oxygens and between nitrogen and oxygen in Kirby's acetal systems were affordable when a strong hydrogen bonding was developed in the products and the corresponding transition states leading to them.

Our previous studies on enzyme models established the necessity to explore the reaction mechanism in order to assign the driving force affecting the reaction rate for a design of an efficient chemical device (prodrug) capable of releasing the parental drug in a programmable manner [10–27]. The prodrugs are designed such that they undergo cleavage reactions in physiological environments (pH 1.5, 6.5 and 7.4) with rates that are completely dependent on the structural features of the inactive linker. A number of linkers could be used to obtain different prodrugs that release the parental drug in different rates that are dependent on the nature or the structural features of the linker.

Continuing our research for utilizing enzyme models as potential linkers for drugs containing hydroxyl groups, we sought to study the mechanism and driving forces affecting the proton transfer rate in some of Kirby's enzyme models (prodrugs linkers). It is expected that such linkers will have a potential to be good carriers to paracetamol. It is worth noting that linking the paracetamol with such linkers *via* its phenolic hydroxyl group will hinder its bitter taste.

Our proposed paracetamol prodrug systems based on proton transfer reactions are illustrated in Scheme 1.

Based on the DFT calculations on the proton transfers in Kirby's enzyme models 1–10 reported herein (Scheme 2), three paracetamol prodrugs are proposed. As shown in Scheme 1, the paracetamol prodrugs, ProD 1–3, have a carboxylic acid group (hydrophilic moiety) and a lipophilic moiety (the rest of the molecule), where the combination of both groups ensures a moderate HLB. It should be noted that the HLB value will be determined upon the physiologic environment by which the prodrug is dissolved. For example, in the stomach, the paracetamol prodrugs will primarily exist in the carboxylic acid form whereas in the blood circulation the carboxylate anion form will be predominant. It is planned that ProD 1–3 will be obtained as sodium or potassium carboxylate salt since this form is expected to be resistant to cleavage by a proton transfer process. The latter is feasible when the carboxylate anion is converted to the free acid form (Scheme 1).

It should be emphasized that prodrugs ProD 1–3 could be used in different dosage forms (tablets, syrups, suppositories, and etc.) because of their potential solubility in organic and aqueous media due to the ability of their carboxyl groups to be converted to the corresponding carboxylate salt.

In this manuscript, we describe our DFT quantum molecular orbital investigations of ground state and transition state structures, vibrational frequencies, and reaction trajectories for intramolecular proton transfer in ten of Kirby's enzyme model systems 1–10 (Scheme 2). It is expected that the calculations study on systems 1–10 will provide a good basis for the prediction of the pharmacokinetic behavior of paracetamol prodrugs of the type ProD 1–3.

## Calculations methods

The DFT calculations at B3LYP/6-31G (d,p) level were carried out using the quantum chemical package Gaussian-98 [53]. The starting geometries of all the molecules presented in this study were obtained using the Argus Lab program [54] and were initially optimized in the presence of one molecule of water at the AM1 level of theory, followed by an optimization at the HF/6-31G level [53]. The calculations were carried out based on the restricted Hartree-Fock (RHF) method with full optimization of all geometrical variables. An energy minimum (a stable compound or a reactive intermediate) has no negative vibrational force constant. A transition state is a saddle point which has only one negative vibrational force constant [55]. The "reaction coordinate method" [56] was used to calculate the activation energy in systems 1–10 and ProD 1–3. In this method, one bond length is constrained for the appropriate degree of freedom while all other variables are freely optimized. The activation energy values for the

**Scheme 1** Proton transfer reactions in ProD 1–3

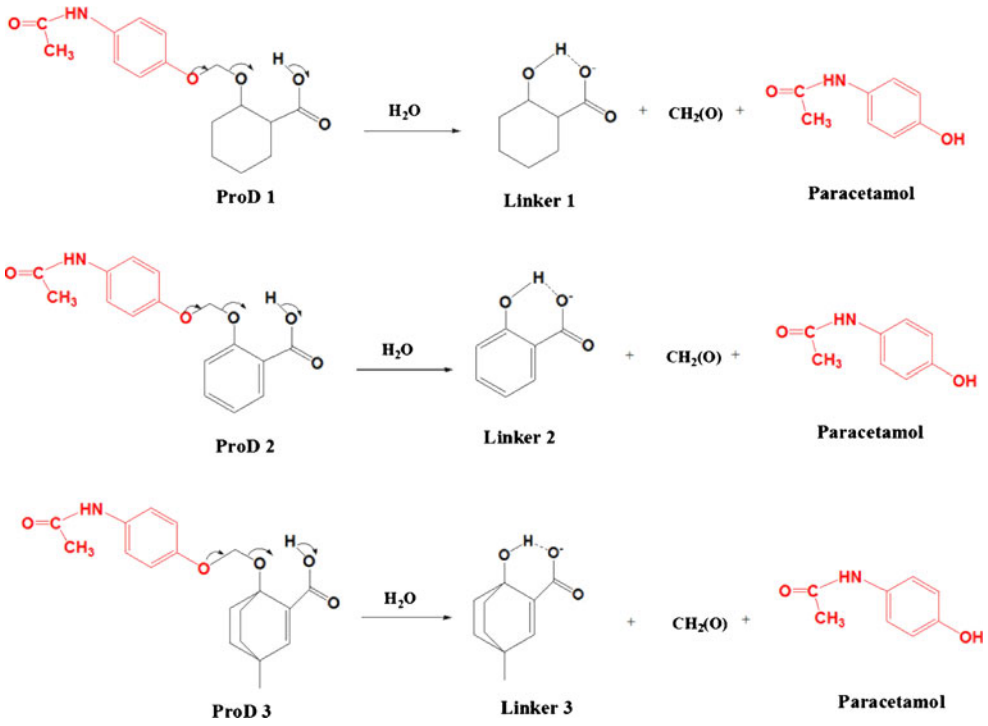


proton transfer reactions were calculated from the difference in energies of the global minimum structures and the derived transition states (TS). Verification of the desired reactants and products was accomplished using the "intrinsic coordinate method" [56]. The transition state structures were verified by their only one negative frequency. Full optimization of the transition states was accomplished after removing any constrains imposed while executing the energy profile. The activation energies obtained from DFT at B3LYP/6-31G (d,p) level of theory for 1–10 and ProD 1–3 were calculated with and without the inclusion of solvent (water). The calculations with the incorporation of a solvent were performed using the integral equation formalism model of the polarizable continuum model (PCM) [57–60].

## Results and discussion

To mask paracetamol bitterness, the pro-drug approach of linking paracetamol to a moiety, which upon dissolution in a physiologic environment, librates the parental drug seems to be promising. Kirby's mechanistic study on acetals that were used as enzyme models has inspired us to exploit these models as appropriate linkers for masking the bitter taste of paracetamol. Kirby's kinetic study on processes 1–10 (Scheme 2) indicates that the rate-limiting step in these processes is a proton transfer from the carboxylic hydroxyl group into the neighboring ether oxygen. In addition, Kirby's findings revealed that the proton transfer rate is largely determined on the strength of the hydrogen bonds in the products and consequently in the transition state leading to them [43–52]. Thus, it is safe to conclude that the proton transfer rate is dependent on the structural features of the enzyme model (linker) as evident from the different experimental rate values measured for processes 1–10.

Replacing the leaving group (methoxy) in the reactants of the linkers 1–10 (Scheme 2) with paracetamol (ProD 1–3, Scheme 1) is not expected to have any significant effect on the rates of the proton transfer in these processes. Therefore, computational investigation of the kinetic properties for these linkers will shed light on the cleavage rates of paracetamol prodrugs ProD 1–3.

### General consideration

Because the energy of carboxylic acid is strongly dependent on its conformation and especially on its ability to be engaged either inter- or intramolecularly in hydrogen bonding, we were concerned with the identification of the most stable conformation (global minimum) for each of Kirby's enzyme models 1–10 and prodrugs ProD 1–3 calculated in this study. This was accomplished by 36 rotations of the carboxyl group about the bond C4-C6 in increments of 10° (i.e., variation of the dihedral angle O5C4C6C7, see Chart 1) and calculation of the energies of the resulting conformers.

In the DFT calculations of the reactants in 1–10 and ProD 1–3, two types of conformers were considered: one in which the carboxylic hydroxyl proton is *syn* to the alkoxy

**Scheme 2** Proton transfer reactions in 1–10, where GM and P are the reactants and products, respectively

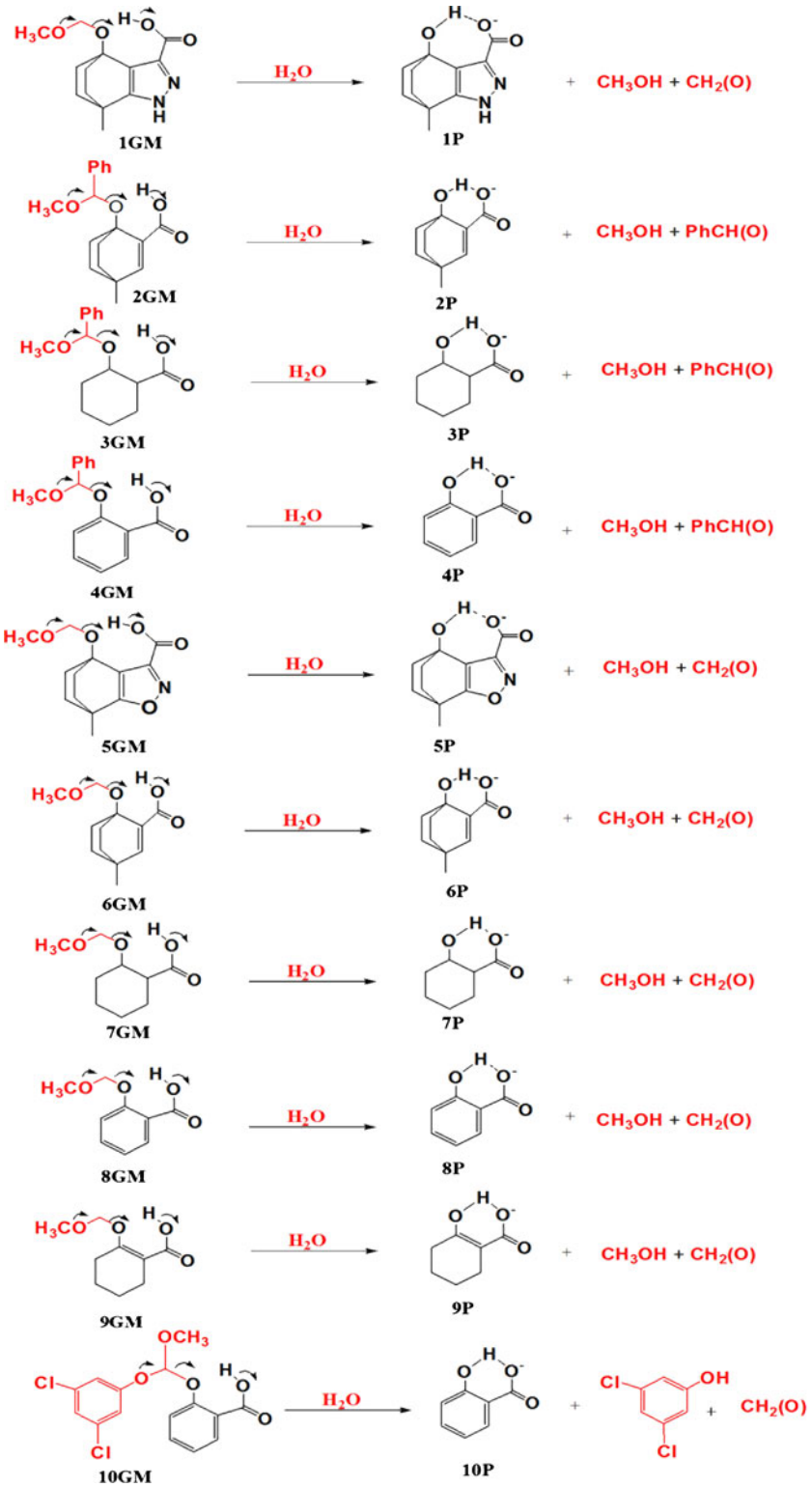


group in the β position of the carboxylic acid moiety (R, see Chart 1) and another in which it is *anti*. It was found that all global minimum structures exhibit a *syn* conformation. Further, the calculation results revealed that in 3, 7, 10 and ProD 1 the global minimum structures reside in a conformation by which the carboxylic hydroxyl proton is far away from the alkoxy oxygen (no hydrogen bonding exists between the carboxylic hydroxyl proton and the alkoxy oxygen) and instead it engages in a hydrogen bonding with a molecule of water (Fig. 1a). For systems 1–2,

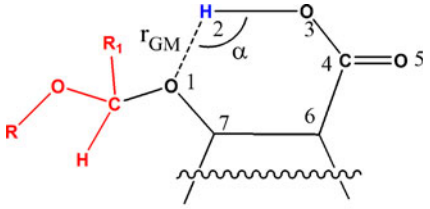


GM

**Chart 1** Schematic representation of the reactants in the proton transfers of Kirby's enzyme models 1–10 and ProD 1–3. GM is the global minimum structure, $r_{GM}$ is the O—H distance in the GM. α, is the angle of attack (hydrogen bonding) O-H-O in the GM

4–6, 8–9, and ProD 2–3, the global minimum conformations were those having intramolecular hydrogen bonding between the carboxylic hydroxyl proton and the alkoxy oxygen (see Fig. 1a).

Structural analysis for the entities involved in the proton transfers of 1–10 and ProD 1–3

*Global minimum structures (GM)*

Generally, reactions in aqueous medium involve interactions between the reactants and water. The nature for such interactions is dependent on the structural features of the reactants. Since the proton transfers in 1–10 were carried out in aqueous medium, we have calculated the geometries of the entities involved in these processes in the presence of one molecule of water followed by optimization in a cluster of water. Figure 1a and Table 1 illustrate the DFT calculated properties for the global minimum structures of 1–10 (1GM-10GM) and ProD 1–3 (ProD 1GM-3GM). Examination of the optimized structures for 1GM-10GM and ProD 1GM-3GM indicate that 3GM, 7GM, 10GM, and ProD 1GM exhibit conformations by which the carboxylic group is engaged intermolecularly in a hydrogen bonding with a molecule of water. This is because the carboxyl group in 3GM, 7GM, 10GM, and ProD 1GM prefers to be engaged in hydrogen bonding with a molecule of water rather than intramolecularly, since the latter is energetically expensive due to a high energy barrier for the rotation of the carboxyl group around the C4-C6 bond [43–52]. It should be indicated that Fife reported that acetal 3GM shows no intramolecular general acid catalysis by the neighboring carboxyl group [61].

On the other hand, 1GM-2GM, 4GM-6GM, 8GM-9GM and ProD 2GM-3GM were found to reside in a conformation by which the carboxylic hydroxyl proton is engaged in an intramolecular hydrogen bond with the neighboring alkoxy oxygen. This engagement results in the formation of a seven-membered ring for 1GM and 5GM and a six-membered ring for 2GM-4GM, 6GM, 8GM, 9GM, ProD 2GM, and ProD 3GM (see Figs. 1a and 2). The DFT calculated hydrogen bonding length ($r_{GM}$) in 3GM, 7GM, 10GM, and ProD 1GM (reactants that are engaged intermolecularly with a water molecule) was found to be in the range of 3.60 Å-3.66 Å and that for the attack angle α (the hydrogen bond angle, O1H2O3) to be in the range of 47°-58°. On the other hand, the $r_{GM}$ and α values for 1GM-10GM and ProD 1GM-3GM were 1.69Å-1.75 Å and 143°-170.7°, respectively. Furthermore, the hydrogen bonding strength, $r_{GM}$ (O1-H2), varies according to the structural features of the starting geometry.

*Transition state structures (TS)*

The DFT calculated geometries for the transition states of 1–10 (1TS-10TS) and ProD 1–3 (ProD 1TS-3TS) are depicted in Figs. 1b and 2 and Table 1. Inspection of the optimized structures for 1TS-10TS and ProD 1TS-3TS revealed that all the TS structures involve strong hydrogen bonding between the carboxylic hydroxyl proton (H2) and the ether oxygen. The calculated hydrogen bonding angle (O1H2O3) in the TS optimized structures was found in the range of 131°-170 °.

*Product geometries (P)*

The DFT calculated geometries for the products of 1–10 (1P-6P) and ProD 1–3 (ProD 1P-3P) shown in Fig. 1c indicate the presence of a strong hydrogen bond between O1H2O3 where the bond length was found in the range 1.45Å to 1.66 Å and the O1H2O3 angle was in the range of 154 ° −170 °. This is similar to that found for the corresponding transition state structures, 1TS-10TS and ProD 1TS-3TS.

Calculations of the kinetic properties for the proton transfer in 1–10 and ProD 1–3

Using the quantum chemical package Gaussian-98 [53] we calculated the DFT at B3LYP/6-31G (d,p) level of theory the kinetic and thermodynamic properties for the intramolecular proton transfer in processes 1–10 and ProD 1–3 (Schemes 1 and 2).

The B3LYP/6-31G (d,p) activation energies were calculated in the presence of one molecule of water and with the inclusion of a cluster of water as a solvent. The calculation results show that the energies with and without a cluster of water are significantly different (Table 2). This indicates that the presence of water as a solvent has a profound effect on the proton transfer rate values. This is in accordance with previously reported studies by Kirby and Fife that show the importance of water in the mechanistic pathway for the proton transfer in such systems [43–52, 61].

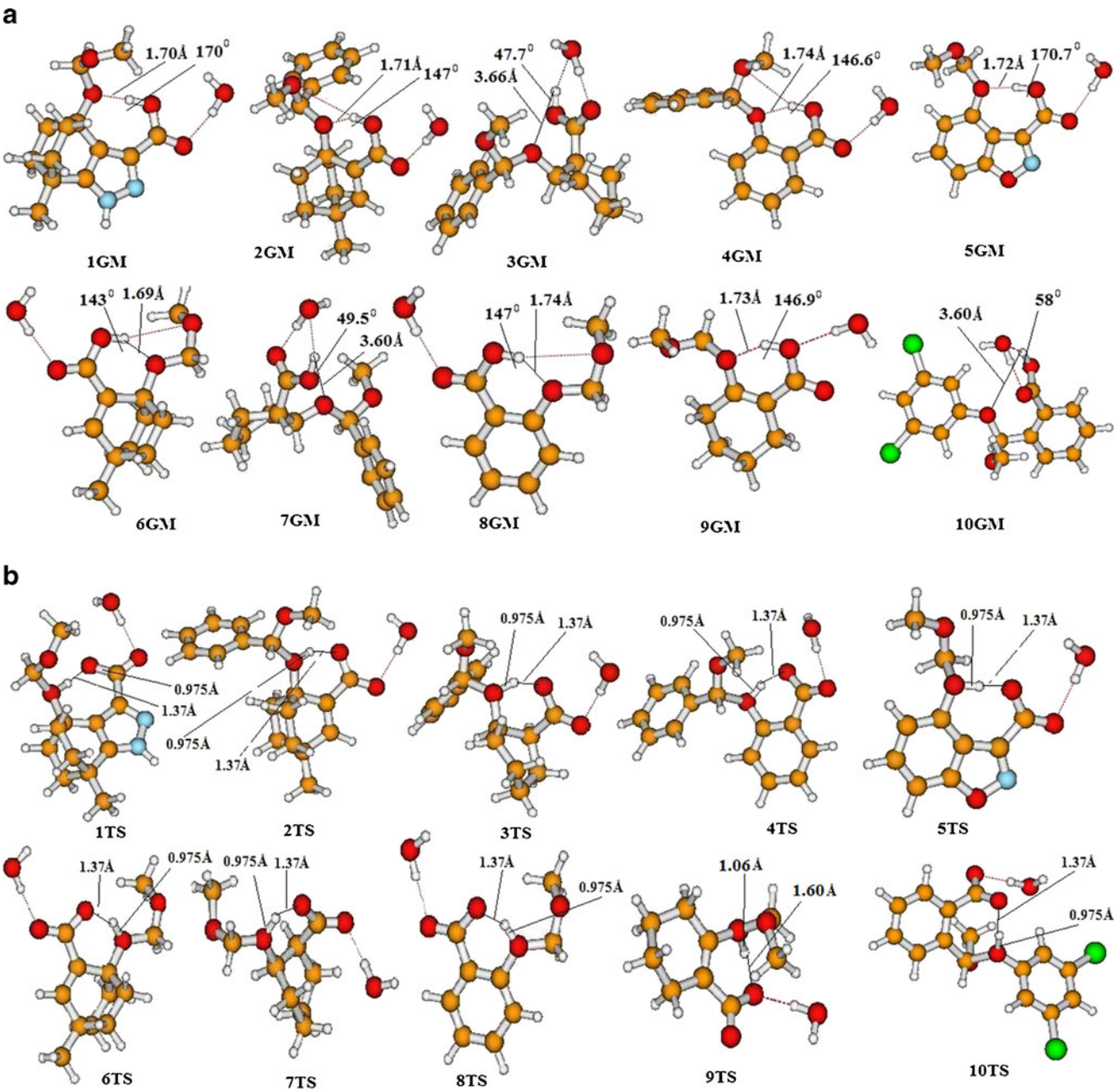


**Fig. 1** (**a**) DFT optimized structures for the global minimum (GM) structures in the intramolecular proton transfer reaction of 1–10. (**b**) DFT optimized structures for the transition state (TS) structures in the intramolecular proton transfer reaction of 1–10. **c** DFT optimized structures for the product (P) structures in the intramolecular proton transfer reaction of 1–10

Using the calculated DFT enthalpic and entropic energies for the global minimum structures 1GM-10GM and ProD 1GM-3GM and their corresponding transition states 1TS-10TS and ProD 1TS-3TS (Table 1) we have calculated the enthalpic ($\Delta H^{\ddagger}$), the entropic ($T\Delta S^{\ddagger}$), and the free activation energies ($\Delta G^{\ddagger}$), in the gas phase and in the presence of cluster of water, for the corresponding proton transfer reactions. The calculated energy values are summarized in Table 2.

*The effect of the distance $r_{GM}$ and the angle $\alpha$ on the activation energy for the proton transfer in processes 1–6*

The intramolecular hydrogen bonding ($r_{GM}$) between the hydroxyl proton (H2) and the ether oxygen O1 (O1-H2) was found to be dependent on the conformation of the global minimum structure. Short $r_{GM}$ values were obtained when the attack angle ($\alpha$) values in the GM conformations

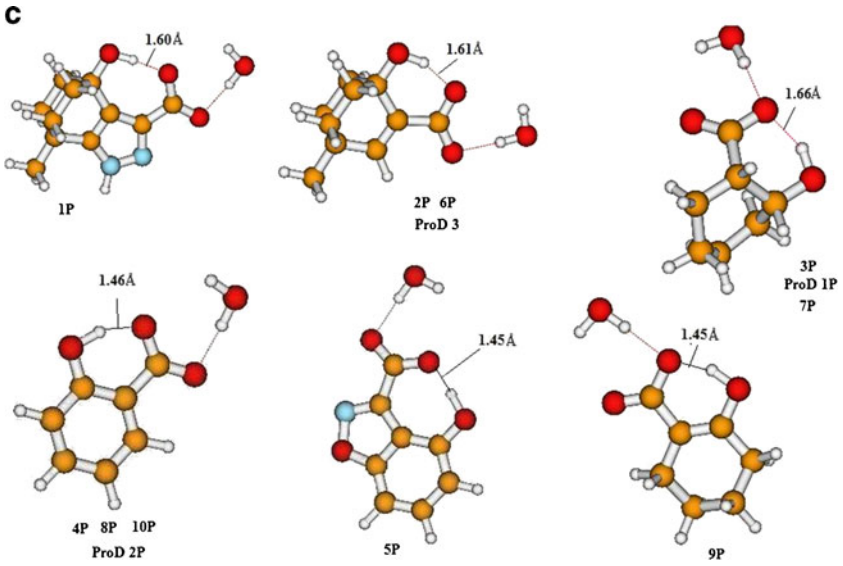


**Fig. 1** (continued)

were high and close to 180°, whereas small α values resulted in longer $r_{GM}$ distances (Figs. 1a and 2). In fact, a strong correlation with a correlation coefficient of R=0.98 was found between the distance $r_{GM}$ and the attack angle α (Fig. 3a).

Examination of Table 2 revealed that the calculated free activation energy ($\Delta G^{\ddagger}$) in the gas phase and in water needed to execute a proton transfer in systems 1–10 and ProD 1–3 is largely affected by both the O1-H2 distance ($r_{GM}$) and the attack angle O1H2O3 (α) (see Chart 1). Acetals having global minimum conformation with low $r_{GM}$ and high α, such as 1, 5, and ProD 3, undergo proton transfer in higher rates (lower $\Delta G^{\ddagger}$) than those having high $r_{GM}$ and low α values, such as 3, 7, and ProD 1. When $r_{GM}$ and α values were examined for correlation with the calculated DFT enthalpic energies ($\Delta H^{\ddagger}$) a linear correlation was found between $\Delta H^{\ddagger}$ and $r_{GM}^2 \times \sin(180-\alpha)$ with a correlation coefficient of R=0.95. On the other hand, a correlation of the activation free energies ($\Delta G^{\ddagger}$) with $r_{GM}^2 \times \sin(180-\alpha)$ gave an R value of 0.85 (Fig. 3b).

The measure generally used for intramolecular efficiency is the effective molarity (EM). The EM parameter is defined as $k_{intra}/k_{inter}$ for corresponding intramolecular and intermolecular processes driven by identical mechanisms.

**Table 1** DFT (B3LYP) calculated properties for the proton transfer reactions of 1–10 and ProD 1-3

| Struct. | Enthalpy, H In Hartree | Entropy, S, Cal/Mol-Kelvin | Frequency $Cm^{-1}$ | Struct. | Enthalpy, H In Hartree | Entropy, S, Cal/Mol-Kelvin | Frequency $Cm^{-1}$ |
|---|---|---|---|---|---|---|---|
| 1GM | -993.05253 | 153.17 | ——— | 8GM | -726.31205 | 132.92 | ——— |
| 1TS | -993.00826 | 144.17 | 181.03i | 8TS | -726.26559 | 119.33 | 132.40i |
| 2GM | -1076.50693 | 172.52 | ——— | 9GM | -728.72138 | 133.20 | ——— |
| 2TS | -1076.45691 | 160.07 | 611.61i | 9TS | -728.66450 | 120.34 | 522.39i |
| 3GM | -957.37381 | 159.64 | ——— | 10GM | -1876.55809 | 152.33 | ——— |
| 3TS | -957.32753 | 142.46 | 184.58i | 10TS | -1876.49684 | 154.58 | 719.08i |
| 4GM | -961.00056 | 152.14 | ——— | ProD 1GM | -1129.71308 | 171.26 | ——— |
| 4TS | -960.93507 | 155.62 | 578.23i | ProD 1TS | -1129.63371 | 160.51 | 612.59i |
| 5GM | -893.73201 | 135.57 | ——— | ProD 2GM | -1126.07858 | 165.90 | ——— |
| 5TS | -893.68532 | 135.66 | 165.49i | ProD 2TS | -1126.02298 | 160.67 | 215.70i |
| 6GM | -845.44633 | 147.15 | ——— | ProD 3GM | -1245.20203 | 173.32 | ——— |
| 6TS | -845.39359 | 142.97 | 558.92i | ProD 3TS | -1245.15174 | 175.96 | 256.26i |
| 7GM | -729.94298 | 129.27 | ——— | ——— | ——— | ——— | ——— |
| 7TS | -729.87241 | 121.80 | 390.28i | ——— | ——— | ——— | ——— |

B3LYP refers to values calculated by B3LYP/6-31G (d, p) in the gas phase. GM and TS are global minimum and transition state structures, respectively

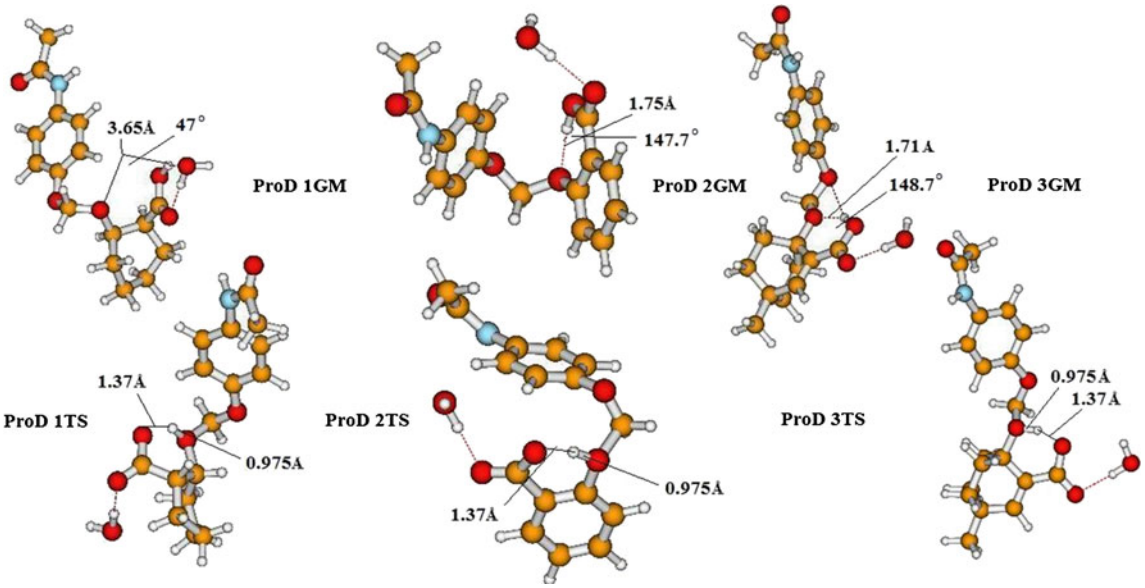


**Fig. 2** DFT optimized global minimum (GM) and transition state structures (TS) for processes ProD 1–3

The factors determining the EM value are ring size, solvent and reaction type. Cyclization reactions *via* intramolecular nucleophilic addition are much more efficient than intramolecular proton transfers. Values in the order of $10^9$-$10^{13}$ M have been measured for the effective molarity in intramolecular processes occurring through nucleophilic addition. Whereas for proton transfer processes values of less than 10 M were obtained [62]. The effective molarity parameter is considered an excellent tool to describe the efficiency of a certain intramolecular process.

In order to obtain credibility for our calculation results we introduce our computation rational for calculating the EM values for processes 1–10 based on the DFT calculated activation energies ($\Delta G^{\ddagger}$) of 1–10 and the corresponding intermolecular process 11 (Scheme 3).

Equation 5 which describes the EM term as a function of the difference in the activation energies of the intra- and the corresponding intermolecular processes was derived from Eqs. 1, 2, 3 and 4. The calculated EM values for processes 1–10 by using Eq. 5 are listed in Table 2.

$$EM = k_{intra}/k_{inter} \tag{1}$$

$$\Delta G^{\ddagger}_{inter} = -RT \ln k_{inter} \tag{2}$$

**Table 2** DFT (B3LYP/6-31G (d,p)) calculated kinetic and thermodynamic properties for the proton transfers in 1–10 and ProD 1-3

| System | log EM[43-52] (exp.) | log EM (calc.) | $\Delta H^{\ddagger}$ (gas phase) | $T\Delta S^{\ddagger}$ (gas phase) | $\Delta G^{\ddagger}$ (gas phase) | $\Delta H^{\ddagger}$ (Water) | $\Delta G^{\ddagger}$ (Water) |
|---|---|---|---|---|---|---|---|
| 1 | 10.000 | 10.58 | 27.78 | -2.68 | 30.46 | 21.47 | 24.15 |
| 2 | 3.4771 | 6.04 | 31.38 | -3.71 | 35.09 | 26.64 | 30.35 |
| 3 | ——— | -0.41 | 41.09 | 1.04 | 40.05 | 40.15 | 39.11 |
| 4 | 3.9777 | 5.30 | 29.04 | -5.12 | 34.16 | 26.22 | 31.34 |
| 5 | 12.600 | 12.72 | 29.30 | 0.03 | 29.27 | 21.22 | 21.19 |
| 6 | ——— | 7.40 | 33.09 | -1.25 | 34.34 | 24.71 | 25.96 |
| 7 | ——— | -1.52 | 44.29 | -2.23 | 46.52 | 34.76 | 36.99 |
| 8 | 4.0000 | 5.17 | 34.32 | -3.42 | 37.74 | 27.53 | 31.52 |
| 9 | 4.3010 | 5.30 | 35.69 | -3.83 | 39.52 | 27.49 | 31.32 |
| 10 | 1.5798 | -1.52 | 38.43 | 0.67 | 37.76 | 37.66 | 36.99 |
| ProD 1 | ——— | -5.81 | 49.80 | -3.20 | 53.00 | 39.65 | 42.85 |
| ProD 2 | ——— | 6.55 | 34.89 | -1.56 | 36.45 | 28.09 | 29.65 |
| ProD 3 | ——— | 11.75 | 31.56 | 0.79 | 29.77 | 23.30 | 22.51 |

$\Delta H^{\ddagger}$ is the activation enthalpic energy (kcal/mol). $T\Delta S^{\ddagger}$ is the activation entropic energy in kcal/mol. $\Delta G^{\ddagger}$ is the activation free energy (kcal/mol).log EM (exp.) and log EM (calc.) are the experimental and calculated effective molarities ($EM = k_{intra}/k_{inter}$)

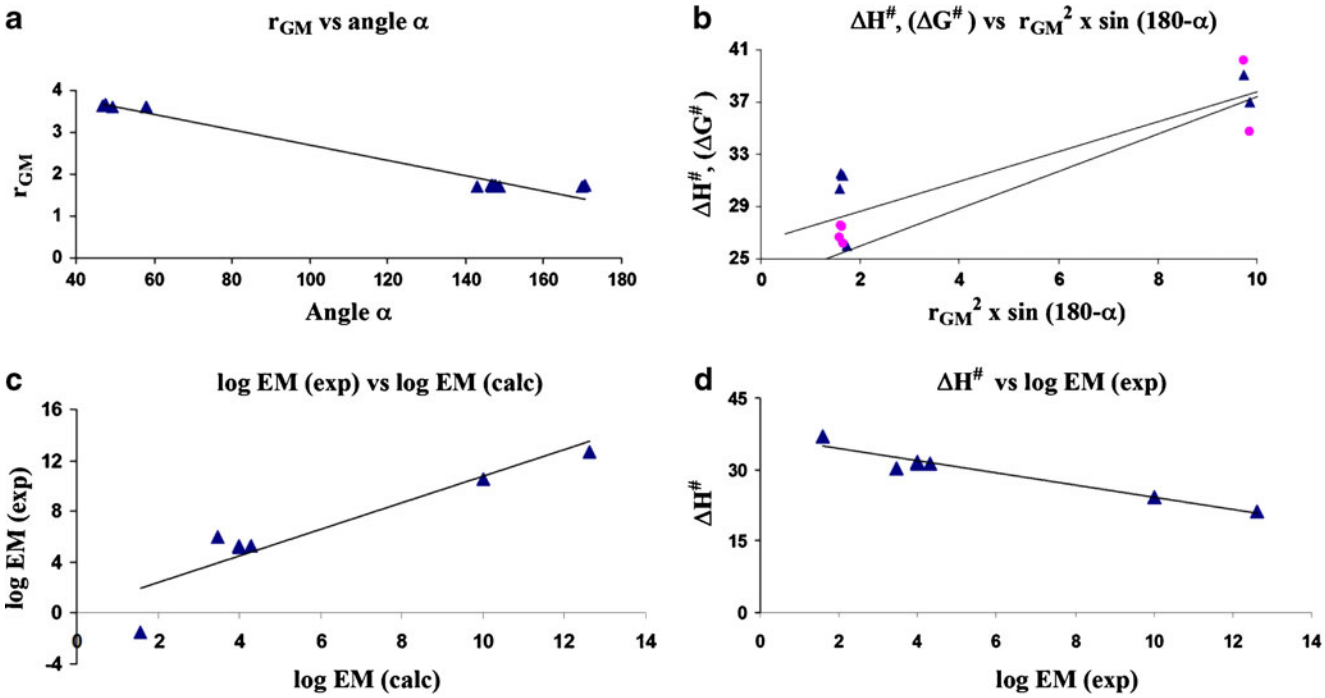


**Fig. 3** (**a**) Plot of the DFT calculated rGM vs. angle α in 1–10 and ProD 1–3, where rGM and α are the distance between the two reactive centers and the attack (hydrogen bond) angle in the GM structure, respectively. (**b**) Plot of the DFT calculated ΔH‡ and ΔG‡ vs. rGM 2×sin (180-α) in 1–10 (**c**) Plot of the experimental EM values vs. the calculated EM values in 1–10 (**d**) Plot of the DFT calculated ΔH‡ values vs. the experimental EM values in 1–10

$$\Delta G^{\ddagger}_{intra} = -RT\ln k_{intra} \quad (3)$$

$$\Delta G^{\ddagger}_{intra} - \Delta G^{\ddagger}_{inter} = -RT(\ln k_{intra}/k_{inter}) \quad (4)$$

$$EM = e^{-(\Delta G\ddagger inter - \Delta G\ddagger intra)/RT}, \quad (5)$$

where T is 298° K and R is the gas constant.

Careful inspection of the effective molarity values shown in Table 2 revealed that systems 1, 5, and ProD 3 are the most efficient processes among 1–10 and ProD 1–3 (log EM >10) and the least efficient are 3, 7, 10, and ProD 1 with log EM <1.6. Furthermore, the calculated EM values were examined for correlation with the experimental EM values. The correlation results show good correlation between the two parameters with a correlation coefficient of R=0.92 (Fig. 3c). Similarly, good correlation results with a correlation coefficient of R=0.97 were obtained when the enthalpic activation energy values were correlated with the experimental EM values (Fig. 3d) [16, 23].

Examination of the calculated EM values for ProD 1–3 (Table 2) indicates that ProD 3 is the process with the highest rate whereas ProD 1 is the process with the lowest rate among the three prodrugs. Based on the experimental $t_{1/2}$ (the time needed for the conversion of 50% of the reactants to products) values for processes 1 and 5 and the EM values for 1, 5, and ProD 1–3 we have calculated the $t_{1/2}$ values for the conversion of the three prodrugs to the parental drug, paracetamol. The calculated $t_{1/2}$ values for ProD 1–3 are 21.3 hours, 4.7 hours and 8 minutes, respectively.

Based on these results solid and liquid preparations of three prodrugs could be made in order to achieve two goals: (1) masking the bitterness of paracetamol and (2) slow release of paracetamol where the rate of the release is determined on the nature of the prodrug linker (Kirby's enzyme model).

**Scheme 3** Intermolecular proton transfer in 11, where GM and P are the reactants and products, respectively

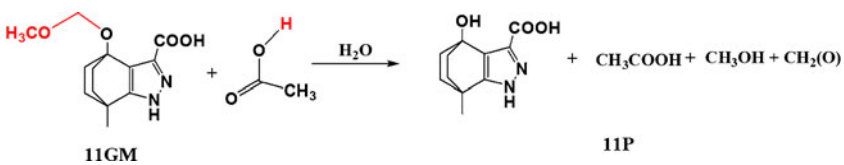


11GM 11P

## Summary and conclusions

The DFT calculation results revealed that the activation energy for the proton transfer in processes 1–10 and ProD 1–3 is quite dependent on the geometric variations in the ground state. It was found that the distance between the two reactive centers, $r_{GM}$, and the angle of attack $\alpha$ are the main factors affecting the rate (activation energy) of the proton transfer. A short distance between the two reactive centers ($r_{GM}$) and hydrogen bonding angle close to 180° result in strong intramolecular hydrogen bonding that clearly indicates the directionality of hydrogen bonding, hence to stabilization of the product and the transition states leading to them and consequently to accelerations in rate.

The linear correlation of the experimental and calculated EM values established a good basis for the design of some paracetamol prodrugs that are capable of masking the bitter taste of paracetamol and have the potential to be used in slow release preparations. Further, this study could be utilized to design other prodrugs by which the rate for the release of the parental drug could be determined according to the nature of the linker (Kirby's enzyme model).

Our future directions include the synthesis of paracetamol prodrugs ProD 1–3 according to known procedures. *in vitro* kinetic studies at different pH values will be made in order to be utilized for the *in vivo* pharmacokinetic studies.

Based on the *in vitro* results, the prodrugs will be tested *in vivo* in addition to paracetamol as a control. The prodrug will be administered to animals by I.V. injection and per-os, blood and urine samples will be collected at different times. The concentration of paracetamol will be determined using a reliable bioanalytical method. Further, pharmacokinetic parameter values will be calculated including oral bioavailability, terminal elimination half-life and other pharmacokinetic parameters as deemed necessary.

**Acknowledgments** The Karaman Co. is thanked for support of our computational facilities. Special thanks are also given to Angi Karaman, Donia Karaman, Rowan Karaman and Nardene Karaman for technical assistance.

## References

1. Remington RWJ (2002) The science and practice of pharmacy, 20th edn. Mack publishing company, Easton, pp 1018–1020
2. Brahmankar DM, Jaiswal SB (1995) Biopharmaceutics & pharmaceutics, 1st edn. Vallabh Prakashan, Delhi, pp 162–165
3. Kuchekar BS, Badhan AC, Mahajan HS (2003) Mouth dissolving tablets: a novel drug delivery system. Pharma Times 35:7–9
4. Ley JP (2008) Masking bitter taste by molecules. Chem Precept Chem Precept 1:58–77
5. Chandreshekar J, Mueller K, Hoon MA, Adler E, Feng L, Guo W, Zuker CS, Ryba NJP (2000) T2Rs function as bitter taste receptor. Cell (Cambridge, Mass) 100:703–711
6. Scotti L, Scotti MT, Ishiki HM, Ferreira MGP, Emerenciano VP, Menezes CMS, Ferreira EI (2007) Quantitative elucidation of the structure-bittereness relationship of cynaropicrin and grosheimin derivatives. Food Chem 105:77–83
7. http://www.assistpainrelief.com/dyn/304/Paracetamol.html
8. http://www.chemicalbook.com/ChemicalProductProperty_EN_CB6141828.htm
9. http://www.chemicalall.com/chemicals-name-a/acetanilide.html
10. Karaman R (2008) Analysis of Menger's spatiotemporal hypothesis. Tetrahedron Lett 49:5998–6002
11. Karaman R (2009) A new mathematical equation relating activation energy to bond angle and distance: a key for understanding the role of acceleration in the lactonization of the trimethyl lock system. Bioorg Chem 37:11–25
12. Karaman R (2009) Reevaluation of Bruice's proximity orientation. Tetrahedron Lett 50:452–456
13. Karaman R (2009) Accelerations in the lactonization of trimethyl lock systems is due to proximity orientation and not to strain effects. Res Lett Org Chem. doi:10.1155/2009/240253, 5 pages
14. Karaman R (2009) The effective molarity (EM) puzzle in proton transfer reactions. Bioorg Chem 37:106–110
15. Karaman R (2009) Cleavage of Menger's aliphatic amide: a model for peptidase enzyme solely explained by proximity orientation in intramolecular proton transfer. J Mol Struct THEOCHEM 910:27–33
16. Karaman R (2009) The *gem*-disubstituent effect-computational study that exposes the relevance of existing theoretical models. Tetrahedron Lett 50:6083–6087
17. Karaman R (2010) Effects of substitution on the effective molarity (EM) for five membered ring-closure reactions- a computational approach. J Mol Struct THEOCHEM 939:69–74
18. Karaman R (2009) Analyzing Kirby's amine olefin – a model for amino-acid ammonia lyases. Tetrahedron Lett 50:7304–7309
19. Karaman R (2010) The effective molarity (EM) puzzle in intramolecular ring-closing reactions. J Mol Struct THEOCHEM 940:70–75
20. Karaman R (2010) The efficiency of proton transfer in Kirby's enzyme model, a computational approach. Tetrahedron Lett 51:2130–2135
21. Karaman R (2010) Proximity vs. strain in ring-closing reactions of bifunctional chain molecules- a computational approach. J Mol Phys 108:1723–1730
22. Karaman R (2010) The effective molarity (EM) – a computational approach. Bioorg Chem 38:165–172
23. Karaman R (2010) A general equation correlating intramolecular rates with "attack" parameters distance and angle. Tetrahedron Lett 51:5185–5190
24. Karaman R, Alfalah S (2010) Multi transition states in SN2 intramolecular reactions. Int Rev Biophys Chem 1:14–23
25. Karaman R, Pascal R (2010) A computational analysis of intramolecularity in proton transfer reactions. Org Bimol Chem 8:5174–5178
26. Karaman R, Hallak H (2010) Anti-malarial pro-drugs- a computational aided design. Chem Biol Drug Des 76:350–360
27. Karaman R (2010) Prodrugs of Aza nucleosides based on proton transfer reactions. J Comput Mol Des 24:961–970
28. Milstein S, Cohen LA (1970) Concurrent general-acid and general-base catalysis of esterification. J Am Chem Soc 92:4377–4382
29. Milstein S, Cohen LA (1970) Rate acceleration by stereopopulation control: models for enzyme action. Proc Natl Acad Sci USA 67:1143–1147
30. Milstein S, Cohen LA (1972) Stereopopulation control. I. Rate enhancement in the lactonizations of o-hydroxyhydrocinnamic acids. J Am Chem Soc 94:9158–9165
31. Menger FM, Ladika M (1990) Remote enzyme-coupled amine release. J Org Chem 35:3006–3007

32. Menger FM, Ladika M (1988) Fast hydrolysis of an aliphatic amide at neutral pH and ambient temperature. A peptidase model. J Am Chem Soc 110:6794–6796
33. Menger FM (1985) On the source of intramolecular and enzymatic reactivity. Acc Chem Res 18:128–134
34. Menger FM, Chow JF, Kaiserman H, Vasquez PC (1983) Directionality of proton transfer in solution. Three systems of known angularity. J Am Chem Soc 105:4996–5002
35. Menger FM (1983) Directionality of organic reactions in solution. Tetrahedron 39:1013–1040
36. Menger FM, Grosssman J, Liotta DC (1983) Transition-state pliability in nitrogen-to-nitrogen proton transfer. J Org Chem 48:905–907
37. Menger FM, Galloway AL, Musaev DG (2003) Relationship between rate and distance. Chem Commun 2370–2371
38. Menger FM (2005) An alternative view of enzyme catalysis. Pure Appl Chem 77:1873–1876, and references therein
39. Bruice TC, Pandit UK (1960) The effect of geminal substitution ring size and rotamer distribution on the intramolecular nucleophilic catalysis of the hydrolysis of monophenyl esters of dibasic acids and the solvolysis of the intermediate anhydrides. J Am Chem Soc 82:5858–5865
40. Bruice TC, Pandit UK (1960) Intramolecular models depicting the kinetic importance of "Fit" in enzymatic catalysis. Proc Natl Acad Sci USA 46:402–404
41. Brown RF, van Gulick NM (1956) The geminal alkyl effect on the rates of ring closure of bromobutylamines. J Org Chem 21:1046–1049
42. Galli C, Mandolini L (2000) The role of ring strain on the ease of ring closure of bifunctional chain molecules. Eur J Org Chem 3117–3125 and references therein
43. Kirby AJ, Parkinson A (1994) Most efficient intramolecular general acid catalysis of acetal hydrolysis by the carboxyl group. J Chem Soc Chem Commun 707–708
44. Brown CJ, Kirby AJ (1997) Efficiency of proton transfer catalysis. Intramolecular general acid catalysis of the hydrolysis of dialkyl acetals of benzaldehyde. J Chem Soc Perkin Trans 2:1081–1093
45. Craze G-A, Kirby AJ (1974) The hydrolysis of substituted 2-methoxymethoxybenzoic acids. J Chem Soc Perkin Trans 2:61–66
46. Barber SE, Dean KES, Kirby AJ (1999) A mechanism for efficient proton-transfer catalysis. Intramolecular general acid catalysis of the hydrolysis of 1-arylethyl ethers of salicylic acid. Can J Chem 792–801
47. Kirby AJ, de Silva MF, Lima D, Roussev CD, Nome F (2006) Efficient intramolecular general acid catalysis of nucleophilic attack on a phosphodiester. J Am Chem Soc 128:16944–16952
48. Kirby AJ, Williams NH (1994) Efficient intramolecular general acid catalysis of enol ether hydrolysis. Hydrogen-bonding stabilization of the transition state for proton transfer to carbon. J Chem Soc Perkin Trans 2:643–648
49. Kirby AJ, Williams NH (1991) Efficient intramolecular general acid catalysis of vinyl ether hydrolysis by the neighbouring carboxylic acid group. J Chem Soc Chem Commun 1643–1644
50. Hartwell E, Hodgson DRW, Kirby AJ (2000) Exploring the limits of efficiency of proton-transfer catalysis in models and enzymes. J Am Chem Soc 122:9326–9327
51. Kirby AJ (1997) Efficiency of proton transfer catalysis in models and enzymes. Acc Chem Res 30:290–296
52. Asaad N, Davies JE, Hodgson DRW, Kirby AJ (2005) The search for efficient intramolecular proton transfer from carbon: the kinetically silent intramolecular general base-catalysed elimination reaction of o-phenyl 8-dimethylamino-1-naphthaldoximes. J Phys Org Chem 18:101–109
53. http://www.gaussian.com
54. Casewit CJ, Colwell KS, Rappe AK (1992) Application of a universal force field to main group compounds. J Am Chem Soc 114:10046–10053
55. Murrell JN, Laidler KJ (1968) Symmetries of activated complexes. Trans Faraday Soc 64:371–377
56. Muller K (1980) Reaction paths on multidimensional energy hypersurfaces. Angew Chem Int Ed Engl 19:1–13
57. Cancès MT, Mennucci B, Tomasi J (1997) A new integral equation formalism for the polarizable continuum model: theoretical background and applications to isotropic and anisotropic dielectrics. J Chem Phys 107:3032–3041
58. Mennucci B, Tomasi J (1997) Coninuum solvation models: a new approach to the problem of solute's charge distribution and cavity boundaries. J Chem Phys 106:5151–5158
59. Mennucci B, Cancès MT, Tomasi J (1997) Evaluation of solvent effects in isotropic and anisotropic dielectrics and in ionic solutions with a unified integral equation method: theoretical bases, computational implementation, and numerical applications. J Phys Chem B 101:10506–10517
60. Tomasi J, Mennucci B, Cancès MT (1997) The IEF version of the PCM solvation method: an overview of a new method addressed to study molecular solutes at the QM *ab initio* level. J Mol Struct THEOCHEM 464:211–226
61. Fife TH, Przystas TJ (1979) Intramolecular general acid catalysis in the hydrolysis of acetals with aliphatic alcohol leaving groups. J Am Chem Soc 101:1202–1210
62. Kirby AJ (2005) Effective molarities for intramolecular reactions. J Phys Org Chem 18:101–278